Charm mixing with $\mathrm{D}^0 \to \mathrm{K}\pi\pi^0$ decays at LHCb

Serena Maccolini
University of Bologna,Italy
under the supervision of Angelo Di Canto (LHCb, CERN)

Abstract

The work here presented reports a first preliminary study of charm mixing using $D^0 \to K^+\pi^-\pi^0$ decays reconstructed in a data sample corresponding to 2 fb^{-1} of integrated luminosity collected by LHCb in 2012. In addition, prospects for Run 2 have been evaluated and are also discussed.

1 Introduction

Charm mixing refers to spontaneous $D^0 \to \bar{D}^0$ and $\bar{D}^0 \to D^0$ transitions occurring in the time evolution of neutral mesons before decaying [9]. This process is a manifestation of flavour-changing neutral currents that occurs because of the charm flavour-defined states, D^0 and $\bar{D}^0$ differ from the physical mass eigenstates, D_1 and D_2, and is characterized by the normalized mass and decay width differences between the two mass eigenstates

$$x = \frac{m_1 - m_2}{\Gamma} \quad \text{and} \quad y = \frac{\Gamma_1 - \Gamma_2}{2\Gamma},$$

where Γ is the average decay width.

Short-range quark-level transitions as well as long-range processes contribute to this phenomenon. The former are governed by loops in which virtual heavy particles are exchanged, making the study of flavour oscillations an attractive area to search for physics beyond the Standard Model. Studies on charm mixing are particularly interesting because it can be sensitive to new physics coupled to the up-type sector.

The first evidence for $D^0 - \bar{D}^0$ oscillation was reported in 2007 by the B-factories [4, 10]. In 2012 the LHCb experiment reported the first observation from a single measurement using decays to the two body $K^+\pi^-$ final state [1]. The current world averages for the mixing parameters, as reported by the *Heavy Flavor Averaging Group* when combining all available mixing measurements [6], do not conclusively show whether x deviates or not from zero. To improve our knowledge of x, it is crucial to study charm mixing with many and different decay channels, and in particular decays to multi-body final states. The goal of this project is to perform, for the first time in LHCb, a preliminary study of charm mixing using $D^0 \to K^+\pi^-\pi^0$ decays.

Charm mixing is here studied by measuring the ratio of $D^0 \to K^+\pi^-\pi^0$ to $D^0 \to K^-\pi^+\pi^0$ decay rates (charge-conjugated decays are implied). The neutral D meson flavour at production time is determined using the charge of the soft (low-momentum) pion π_S in the flavour-conserving $D^{*\pm} \to \overset{(-)}{D}{}^0\pi_S^\pm$ decay. The $D^{*+} \to D^0(\to K^-\pi^+\pi^0)\pi_S^+$ process is referred to as right-sign (RS), whereas the $D^{*+} \to D^0(\to K^+\pi^-\pi^0)\pi_S^+$ is designated as wrong-sign (WS). As graphically shown in Fig. 1, the RS process is dominated by a Cabibbo-favoured (CF) decay amplitude, whereas the WS amplitude includes contributions from both the direct double-Cabibbo-suppressed (DCS) $D^0(\to K^+\pi^-\pi^0)$ decay, as well as $D^0 - \bar{D}^0$ mixing followed by the CF $\bar{D}^0(\to K^+\pi^-\pi^0)$ decay. Since the observed mixing parameters are small [6], the time-dependent ratio $R(t)$ of WS to RS

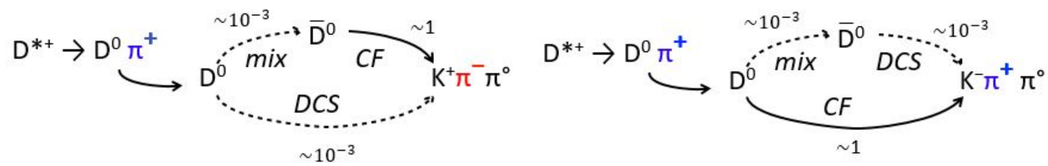

(a) (b)

Figure 1: Scheme of WS (a) and RS (b) decays whereas the $D^* \to D^0(\to K\pi\pi^0)\pi_S$. In the figures each decay.

decays rates, assuming negligible CP violation, can be approximated by the following quadratic expression:

$$R(t) = \frac{WS(t)}{RS(t)} \approx R_D + \alpha\sqrt{R_D}y'\left(\frac{t}{\tau}\right) + \frac{R_M}{2}\left(\frac{t}{\tau}\right)^2 \tag{1}$$

where t/τ is the decay time expressed in units of the average D^0 lifetime. The time-independent term R_D corresponds to the ratio of DCS to CF decay rates integrated over the Dalitz space. The quadratic term is proportional to the mixing rate $R_M = (x^2 + y^2)/2$, which is instead independent of the Dalitz space. The linear term is due to the interference between the DCS and the mixing amplitudes. Here $y' = y\cos(\delta) - x\sin(\delta)$ with δ being a Dalitz-integrated strong phase difference between the DCS and the CF amplitudes, while $0 \le \alpha \le 1$ is the coherence factor and accounts for strong-phase variations over the Dalitz space. In this channel the coherence factor is measured to be 0.82 ± 0.07 [**?**], so large enough to make this channel particularly interesting for mixing studies since the sensitivity to mixing comes mostly from linear term in decay time.

The available experimental measurements of mixing using $D^0 \to K^+\pi^-\pi^0$ come from the B-factories experiments: Belle measures only the time- and Dalitz-integrated ratio R [11]; BaBar has two results, the first measures R and the Dalitz-integrated quantities R_D, $\alpha y'$ and R_M [3], the second measures the mixing parameters x', y' using a time- and Dalitz-dependent analysis [5].

2 Overview of the project

The first task of the project is the selection of the candidates described in § 3. Afterwards in § 4 a BDT selection is implemented and the so-called overlapped WS events are removed with the aim to suppress the background, mainly composed by wrong-π_S candidates. The yields of RS and WS signal are extracted by fitting the $M_{D^0\pi_S}$ distribution and the time- and Dalitz-integrated WS-to-RS ratio is measured in § 5. An estimation in sensitivity with Dalitz-integrated analysis is performed in § 6 where phase-space efficiency and systematic errors are not taken into account. The last task piece of the work is described in **??** and is a view into Run2 data where the impact of new triggers at HLT1 and HLT2 is studied.

3 Reconstruction of $\mathbf{D^0 \to K\pi\pi^0}$ decays

The analysis is based on pp collisions data collected by LHCb during 2012 and corresponding to an integrated luminosity of $2\,\mathrm{fb}^{-1}$.

First explain trigger selection (and hence add a comment on the unavailability of the HLT2 trigger in 2012), then explain the offline candidate reconstruction The LHCb [**?** , XXX]etector is a single-arm forward spectrometer, designed for the study of particles containing b or c quarks. The trigger [**?**] consists of a hardware stage, based on information from the calorimeter and muon systems followed by a first software stage (L0), in which all hight-p_T charged particles are reconstructed. Two software trigger selections are combined for this analysis: HLT1 which is activated if one displaced hight-p_T track is found and HLT2 where a $D^\star$ candidate is included in the reconstruction of the event given by two charged tracks and a deposit of energy in the calorimeter corresponding to a π^0.

Offline, candidate $D^0 \to K^{\pm}\pi^{\mp}\pi^0$ decays are reconstructed by first selecting two charged tracks, consistent with being a kaon and a pion, forming a vertex that is well displaced from the primary pp interaction vertex. These are then combined with a $\pi^0 \to \gamma\gamma$ candidate to form a candidate D^0 decay. The neutral pions are distinguished in resolved and merged candidates according to whether the two photons from their decay result or not in well separated energy clusters in the electromagnetic calorimeter. Resolved neutral pions have better momentum resolution and cover different regions than merged π^0 candidates. For these reasons resolved and merged candidates are treated separately in the analysis. Candidate D^0 decays, that are consistent with originating from the primary vertex, are then combined with a charged low-momentum track to form a $D^{*+} \to D^0\pi^+$ decay. Finally, to improve mass resolution, a kinematical fit of the full decay topology is performed [8] by requiring that the $D^0\pi_S$ vertex to be consistent with the primary vertex and by constraining the reconstructed π^0 mass to its known value [9]. An additional fit, where also the reconstructed D^0 mass is required to be consistent with its known value [9], is used when looking at the Dalitz-plot distribution to ensure that the reconstructed events lie within the allowed kinematical region.

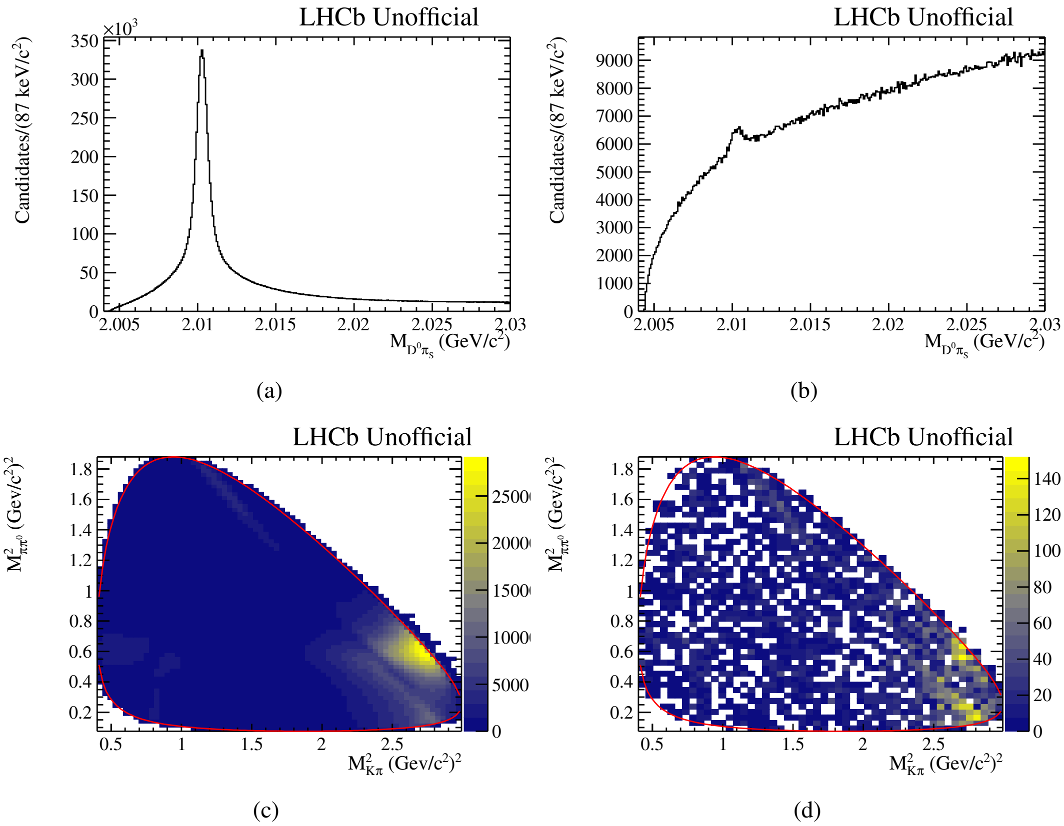

Figure 2: RS (a,c) and WS (b,d) decays for resolved π^0. In (d) the large background has been routhly removed.

Figure 2 (3) shows the $D^0\pi_s$-mass and Dalitz-plot distributions for the selected candidates with resolved (merged) neutral pions, when the reconstructed D^0 mass is constrained to be in the range $[1825,\, 1910]$ MeV/c^2 ($[1800,\, 1950]$ MeV/c^2), corresponding to approximately two times the mass resolution. In the RS sample the signal peak stands clearly over the background that is mainly composed by candidates where a correctly reconstructed D^0 is accidentally paired to a random soft pion from the primary vertex. Since WS events are rarer, the background contribution there is larger. Report the yields for the different samples... The number of RS and WS candidates, obtained after this first selection is $1.27 \cdot 10^7$ ($2.13 \cdot 10^6$) and $3.81 \cdot 10^6$ ($3.28 \cdot 10^5$) for resolved (merged) π^0 sample.

From the plots one can also see that the merged π^0 candidates, despite having a worse mass resolution, show a better signal-to-background ratio. This is because, in average, D^0 candidates made with

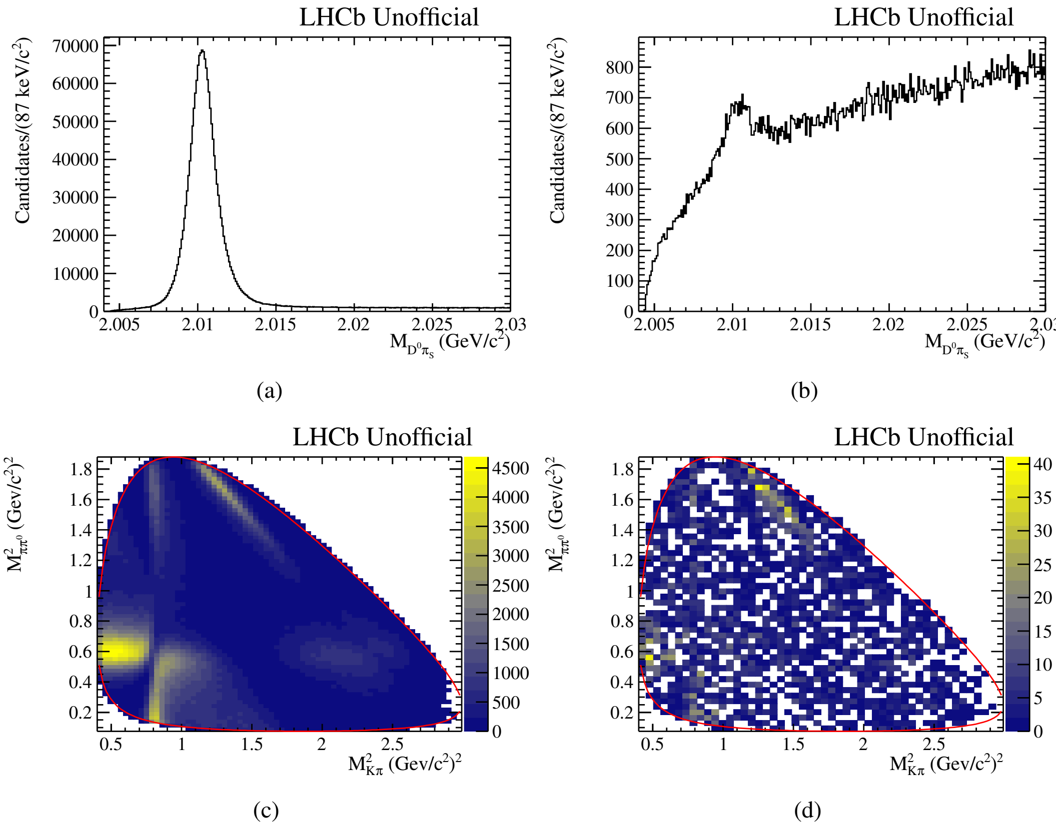

Figure 3: RS (a,c) and WS (b,d) decays for merged π^0. In (d) the large background has been routhly removed.

merged π^0 decays have a larger momentum than resolved ones and therefore suffer from a smaller contamination from background due to randomly-associated low momentum soft pions.

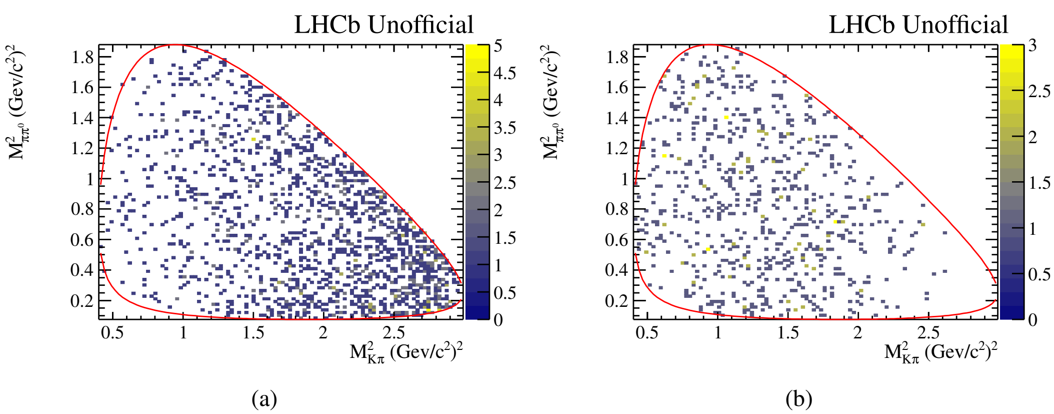

Figure 4: Phase-space RS decays for resolved (a) and merged (b) π^0. Monte Carlo data has been exploited.

The different kinematic coverage between merged and resolved candidates can also be seen from the two complementary Dalitz-plot distributions at Fig. 2 (c) and Fig. 3 (c) where is possible to identify all the intermediate resonances in the decay. This is confirmed by looking at Fig. 4, where the efficiency variation as determined on simulation is shown. Consider both the samples permits at first to neglect efficiency corrections.

4 Suppression of the random-pion background

To suppress the large background of random-pion candidates present in the WS sample a multivariate-analysis selection, based on the *Boosted Decision Tree* (BDT) method of the *Toolkit for Multivariate Data Analysis* [7], has been implemented.

Variable	$< S^2 >$
$p_T(D^0)$	8.3%
$cos\theta_{XY}(p_{K\pi}\text{vs}p_{\pi^0})$	6.5%
$CL(\pi^0)$	4.8%
$P(\pi_S \to \pi)$	3.0%
DTF_Vχ^2	2.5%

(a)

Variable	$< S^2 >$
$p_T(\pi_S)$	7.4%
$P(\pi_S \to \pi)$	6.7%
$p(\pi_S)$	1.6%
DTF_Vχ^2	0.1%

(b)

Table 1: Variables used as input for the MVA training, ordered by their separation power, for resolved (a) and merged (b) π^0 sample. Kinematical variables include: the particle momentum p, the transverse momentum p_T and the cosine of angle θ between $p(K\pi)$ and $p(\pi^0)$ in XY plane. Particle-id variables, based on RICH and calorimeter informations, include: the probability for the identified X particle to be an X particle and the confidence level for the π^0 actually be a π^0. The χ^2 of the D^* vertex from the fit of the topology of the decay (DTF) [8**?**], normalized to the number of degrees of freedom, is a geometric variable.

The BDT is trained with signal and background samples derived directly from data. In particular, RS candidates share the same kinematical and topological properties of the WS candidates, with the only exception of the decay time distribution. The signal and background samples are defined by requiring $|M_{D^0\pi_S} - M_{D*}| < 0.002\,\text{GeV}/c^2$ and $2.02 < M_{D^0\pi_S} < 2.03\,\text{GeV}/c^2$ respectively. A long list of input variables have been studied trying to identify those able to better discriminate signal and background, but also with a low correlation with $M_{D^0\pi_S}$ and Dalitz-plot variables. The discrimination between signal and background is estimated computing for each variable y using the statistical separation $< S^2 >$, defined as

$$< S^2(y) >= \frac{1}{2}\int \frac{(\text{pdf}_S(y) - \text{pdf}_B(y))^2}{\text{pdf}_S(y) + \text{pdf}_B(y)} dy \tag{2}$$

where $\text{pdf}_{S,B}$ are the signal and background probability density functions of the variable under study. The final set that have been chosen is listed in Tab. 1 and comprises variables related to the kinematic of the decay, to the identification of the particles and to the decay topology.

The resulting BDT distributions for signal and background are shown in Fig. 5 while the corresponding signal versus background separation is estimated to be 18.4% (15.1%) for the resolved (merged) π^0 sample. Figure 5 also shows the overtraining check for the BDT: it tests that the distributions produced in BDT training are compatible with those obtained in an independent test sample.

To ensure no bias in the background mass shape after BDT selection, a check on the correlation of BDT with the mass $M_{D^0\pi_S}$ and Dalitz plot has been performed. As shown in Figs. 6 and 7, the correlation is small.

The optimal BDT requirement is chosen as that producing the smallest uncertainty on the measured time-integrated WS-to-RS ratio R. Therefore, many BDT requirements are tested. For each, the number of WS and RS candidates is measured by fitting the obtained $M_{D^0\pi_S}$ distributions (details on the fit are presented later), and their ratio is calculated. Figure 8 shows the uncertainty on R as a function of the BDT cut. In the resolved sample, a minimum is visible for BDT > 0.09, corresponding to about 20% improvement in precision with respect to the case where no BDT selection is applied. Only a marginal gain in resolution is observed for the merged sample, where BDT > -0.10 is chosen, suggesting that this sample is already pure enough for the purposes of our study.

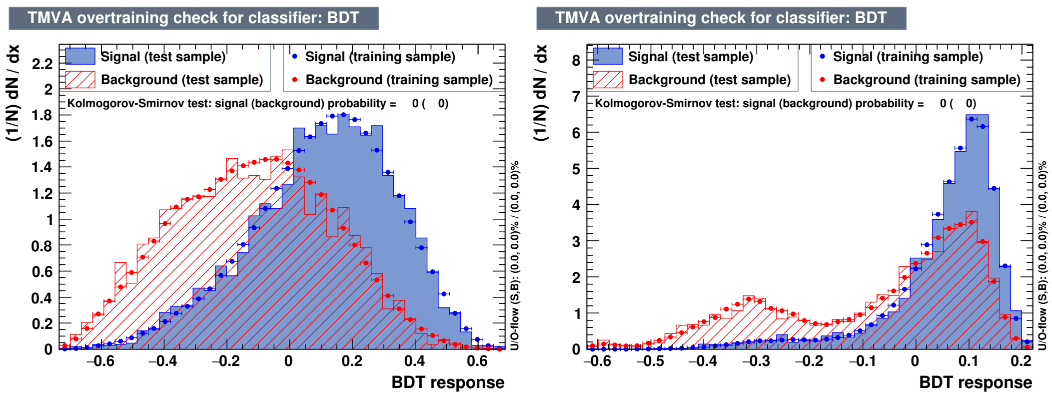

(a) (b)

Figure 5: BDT distributions of RS decays for resolved (a) and merged (b) π^0 sample.

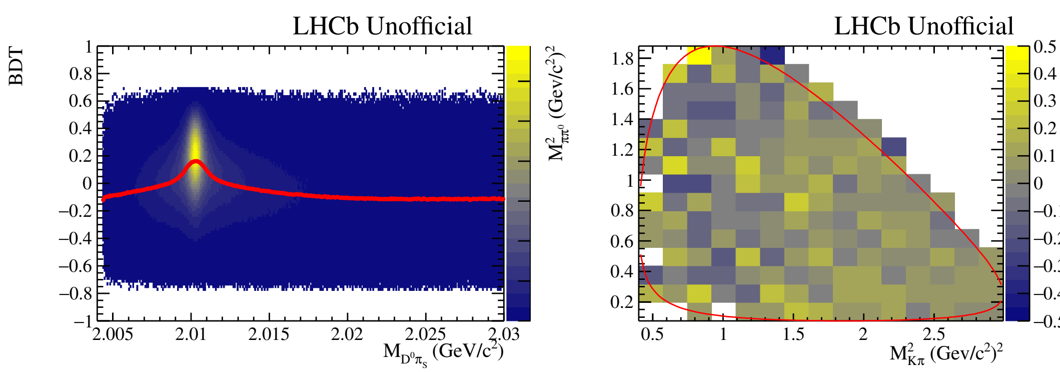

(a) (b)

Figure 6: BDT correlation with $M_{D^0\pi_S}$ (a) and Dalitz plot (b) of RS decays for resolved π^0 sample. In (b) Monte Carlo data has been exploited and <BDT> is represented along the Z axis.

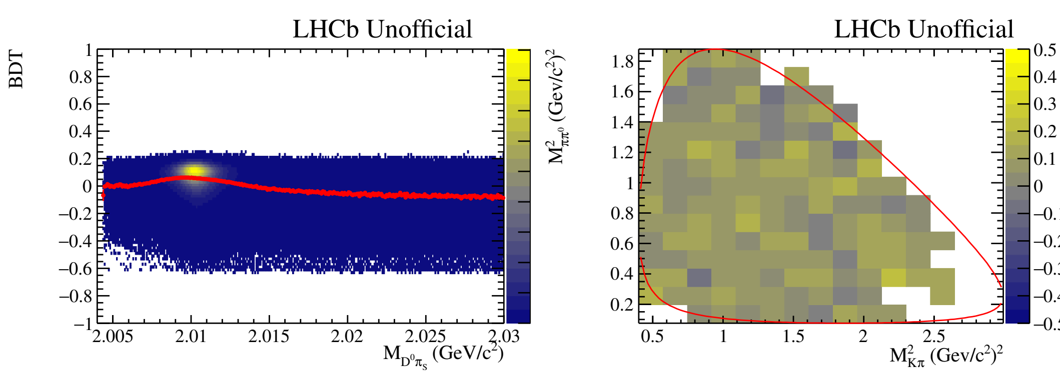

(a) (b)

Figure 7: BDT correlation with $M_{D^0\pi_S}$ (a) and Dalitz plot (b) of RS decays for merged π^0 sample. In (b) Monte Carlo data has been exploited and <BDT> is represented along the Z axis.

An additional 20% (10%) background reduction is achieved by removing the WS candidates, whose D^0 was also used to reconstruct a good RS candidate for resolved (merged) π^0 sample. These candidates are most likely fake WS candidates where a wrong-sign π_s has been mistakenly associated

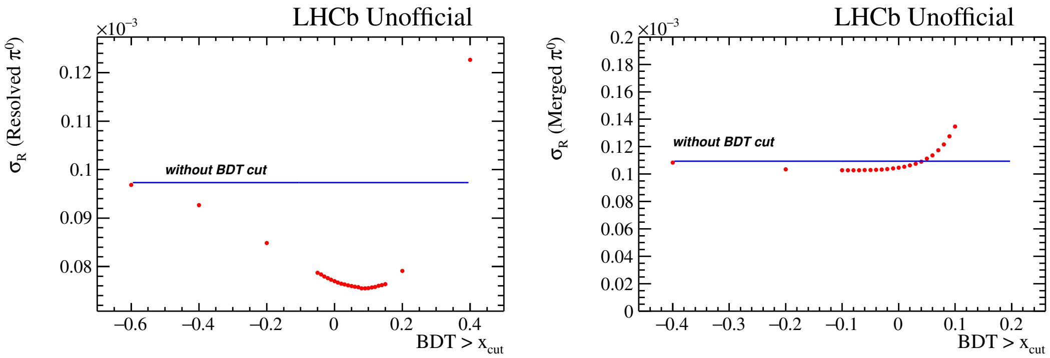

(a) (b)

Figure 8: σ_R in BDTcut for resolved (a) and merged (b) π^0 sample.

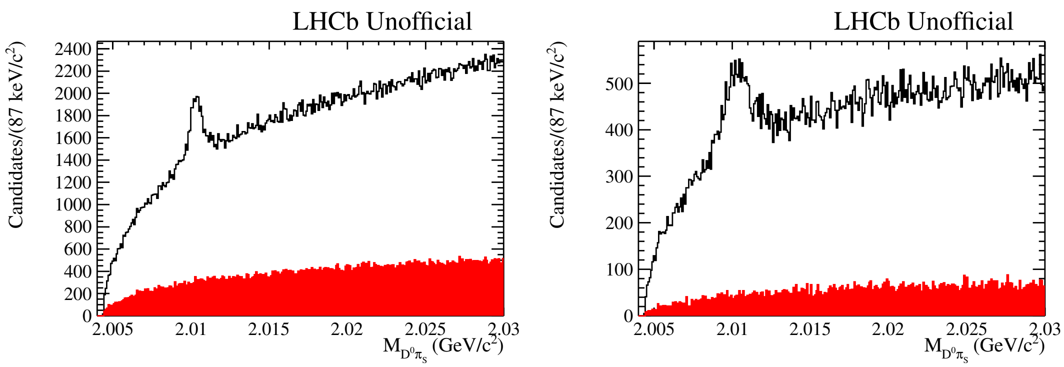

(a) (b)

Figure 9: $M_{D^0\pi_S}$ distributions after the BDT selection of WS events for resolved (a) and merged (b) π^0 sample. In red overlapped candidates.

to the correctly reconstructed $D^0 \to K^-\pi^+$ candidate. Figure 9 shows the $D^0\pi_s$-mass distribution of the removed candidates in comparison with the distribution of the candidates that are retained. The removed candidates do not show any peaking signal-like structure, as expected.

5 Time-integrated analysis

A binned χ^2 fit to the $M_{D^0\pi_S}$ distribution of the finally selected candidates determines the WS and RS signal yields and their ratio. In this fit the signal shape consists of a linear combination of three Gaussian functions and a Johnson SU [**?**] distribution:

$$\text{pdf}_S = f_0 \cdot J_{SU}(m|\mu,\delta,\lambda,\epsilon,\gamma) + f_1 \cdot G_1(m|\mu_1,\sigma_1) + f_2 \cdot G_2(m|\mu_2,\sigma_2) + f_3 \cdot G_3(m|\mu_3,\sigma_3) \quad (3)$$

The background mass shape is parameterized using the function

$$\text{pdf}_B = (m - m_0)^\alpha e^{\beta(m-m_0)}, \quad (4)$$

with m_0 fixed to the threshold value of $m_{D^0} + m_\pi = 2.004\,\text{GeV/c}^2$ [9]. All functions are properly normalized within the fit range going from the threshold up to 2.03 GeV/c^2.

The fit is first performed on the RS sample with all parameters free to float. This allows to accurately determine the signal shape on the very pure and abundant RS decays. The signal shape is then fixed in the subsequent fit to the WS sample.

Figure 10 and 11 show the time-integarted $D^0\pi_s$-mass distributions with fit projections overlaid. The resulting RS and WS yields are $(3.7758 \pm 0.0065) \cdot 10^6$ ($(1.5847 \pm 0.0035) \cdot 10^6$) and $(1.024 \pm$

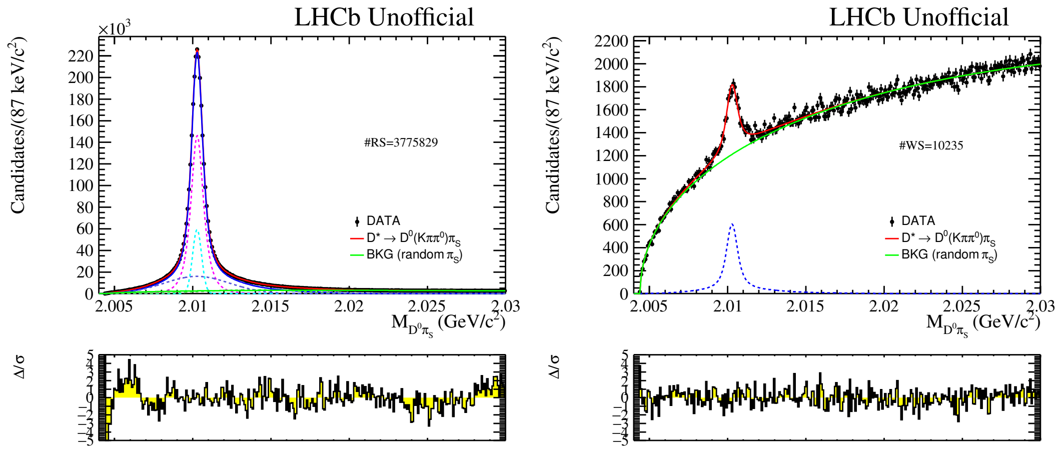

(a) (b)

Figure 10: RS (a) and WS (b) candidates for resolved π^0 sample.

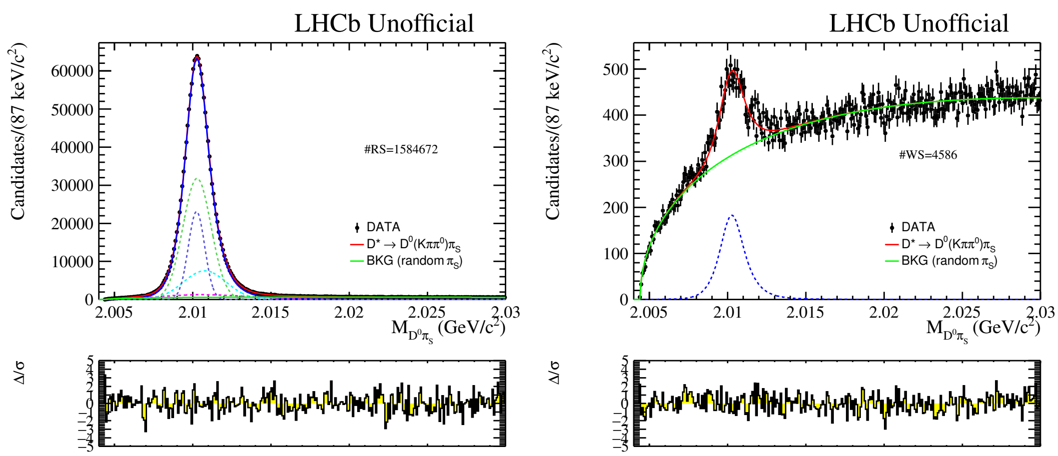

(a) (b)

Figure 11: RS (a) and WS (b) candidates for merged π^0 sample.

$0.027) \cdot 10^4$ ($(4.59 \pm 0.16) \cdot 10^3$) for resolved (merged) π^0 sample. These correspond to about five times more signal candidates than what available in the full sample collected by the BaBar experiment [3].

6 Time-dependent analysis

The samples have been divided in bins of time with about the same statistic. The mass fit is repeated in each subsample with the same procedure as outlined above. Figure 12 show the resulting WS-to-RS ratio as a function of decay time.

The distribution is fit first with a constant (no-mixing hypothesis) and then with Eq. 1 (mixing-allowed hypothesis). The results are shown in Tab. 6. By comparing the results of the two fits, the no-mixing hypothesis is excluded with a p-value of XXX, corresponding to approximately 3.3 Gaussian standard deviations. This is the first evidence of mixing in $K\pi\pi^0$ channel at LHCb.

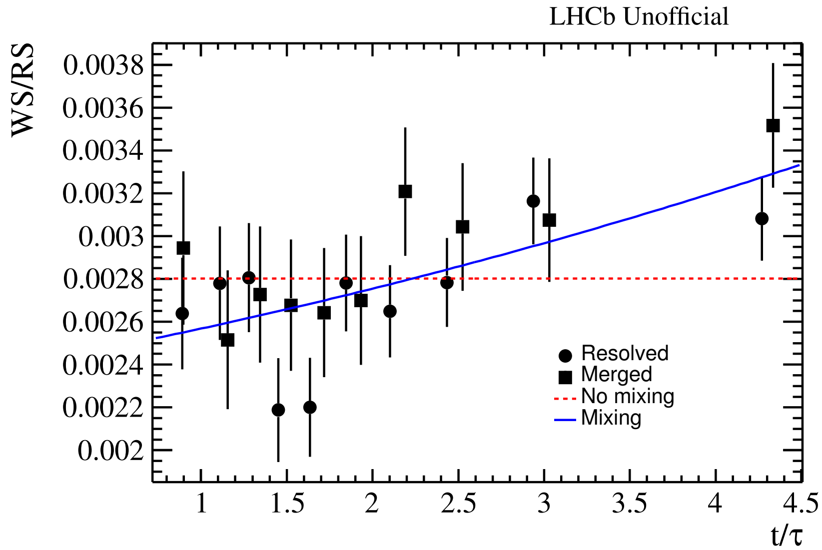

Figure 12: Time-dependent WS/RS ratio.

Parameter	Fit result
R	$(0.2802 \pm 0.0058)\%$
χ^2_0/NDF	30.3/19
R_D	$(0.241 \pm 0.034)\%$
$\alpha y'$	$(0.30 \pm 0.62)\%$
$(x^2 + y^2)/4$	$(0.0013 \pm 0.0055)\%$
χ^2_2/NDF	16.1/17

7 Prospects for Run 2

With the start of Run 2 the LHCb trigger has gone through substantial changes XXX. Of particular interest for the decay channel here discussed are the introduction at HLT1 of new one- and two-charged-track lines based on a multivariate discriminant, and the introduction at HLT2 of an inclusive D^* trigger based on a BDT. By the end of 2015, the inclusive D^* line has been complemented with the implementation of a set of exclusive $D^{*+} \to D^0(\to K^\pm\pi^\mp\pi^0)\pi^+$ lines (including both resolved and merged $\pi^0 \to \gamma\gamma$ decays).

Year	N_{RS}/L (fb)	$\frac{N_{RS}/L(2012)}{N_{RS}/L(year)}$
2012	2'700'000	1
2015	6'440'000	2.4
2016	5'710'000	2.1

Table 2: Number of RS signal candidates per integrated luminosity collected during the years.

Table 2 shows xxx. The increase in signal yield per integrated luminosity is partially due to the larger available production cross-section at 13 TeV with respect to 7 TeV (which for charm mesons is measured to be approximately two times larger [2]) and partially to the trigger improvements. Small differences between 2015 and 2016 are expected due to different trigger thresholds and data-taking conditions.

Table 3 reports the breakdown of the selected RS signal yields in 2016 in terms of the different trigger lines at HLT1 and HLT2. At HLT1 most of the candidates are selected by the one-track line with approximately 2% (5%) of the resolved (merged) candidates are selected only through the two-track line. At HLT2, the improvement induced by the exclusive line is more evident. In particular, about 11% (50%) of the resolved (merged) candidates are selected only by the exclusive line.

	Resolved	Merged
All candidates	$(1.5631 \pm 0.0055) \cdot 10^6$	$(4.5 \pm 0.21) \cdot 10^3$
HLT1TrackMVA	$(1.5626 \pm 0.0055) \cdot 10^6$	$(4.5 \pm 0.21) \cdot 10^3$
HLT1TwoTrackMVA	$(1.3811 \pm 0.0052) \cdot 10^6$	$(3.96 \pm 0.20) \cdot 10^2$
HLT2Inclusive	$(1.5631 \pm 0.0055) \cdot 10^6$	$(4.5 \pm 0.21) \cdot 10^3$
HLT2Exclusive	$(2.919 \pm 0.021) \cdot 10^4$	$(1.01 \pm 0.18) \cdot 10^2$

Table 3: Yields resolved (a) merged (b) 2016.

Conclusion

In summary, this work represents a first attempt to measure $D^0 - \bar{D}^0$ mixing using $D^0 \to K^{\pm}\pi^{\mp}\pi^0$ decays at LHCb. The obtained results, based on a time-dependent and Dalitz-integrated measurement of the WS-to-RS yield ratio in 2012 data, seem to be competitive with other available measurements based on these decays [11, 3, 5]. However, all results presented have to be considered preliminary and unofficial. The sensitivity to the mixing parameters could be increased with the larger statistics that is being collected during Run 2 and/or through a more sophisticated time- and Dalitz-plot-dependent analysis. For the work here presented, I have been awarded by the LHCb collaboration with the Moritz Karbach prize for outstanding summer students.

References

[1] R Aaij et al. Observation of $D^0 - \overline{D}^0$ oscillations. *Phys. Rev. Lett.*, 110(10):101802, 2013.

[2] Roel Aaij et al. Measurements of prompt charm production cross-sections in pp collisions at $\sqrt{s} = 13$ TeV. *JHEP*, 03:159, 2016. [Erratum: JHEP09,013(2016)].

[3] Bernard Aubert et al. Search for D^0 -anti-D0 Mixing and Branching-Ratio Measurement in the Decay $D^0 \to K^+\pi^-\pi^0$. *Phys. Rev. Lett.*, 97:221803, 2006.

[4] Bernard Aubert et al. Evidence for D^0 -anti-D^0 Mixing. *Phys. Rev. Lett.*, 98:211802, 2007.

[5] Bernard Aubert et al. Measurement of $D^0 - \bar{D}^0$ mixing from a time-dependent amplitude analysis of $D^0 \to K^+\pi^-\pi^0$ decays. *Phys. Rev. Lett.*, 103:211801, 2009.

[6] Heavy Flavor Averaging Group.

[7] A. Hoecker, P. Speckmayer, J. Stelzer, J. Therhaag, E. von Toerne, H. Voss, M. Backes, T. Carli, O. Cohen, A. Christov, D. Dannheim, K. Danielowski, S. Henrot-Versille, M. Jachowski, K. Kraszewski, A. Krasznahorkay, Jr., M. Kruk, Y. Mahalalel, R. Ospanov, X. Prudent, A. Robert, D. Schouten, F. Tegenfeldt, A. Voigt, K. Voss, M. Wolter, and A. Zemla. TMVA - Toolkit for Multivariate Data Analysis. *ArXiv Physics e-prints*, March 2007.

[8] W. D. Hulsbergen. Decay chain fitting with a Kalman filter. *Nuclear Instruments and Methods in Physics Research A*, 552:566–575, November 2005.

[9] K. A. Olive et al. Review of Particle Physics. *Chin. Phys.*, C38:090001, 2014.

[10] M. Starič et al. Evidence for D^0-$\bar{D}^0$ mixing. *Phys. Rev. Lett.*, 98:211803, May 2007.

[11] X. C. Tian et al. Measurement of the wrong-sign decays D0 —¿ K+ pi- (pi0, pi+ pi-) and search for CP violation. *Phys. Rev. Lett.*, 95:231801, 2005.